Indonesian Journal of Electronics, Electromedical Engineering, and Medical Informatics
Homepage: ijeeemi.org; Vol. 7, No. 1, pp. 11-22, February 2025; e-ISSN: 2656-8624.
https://doi.org/10.35882/ijeeemi.v7i1.46

RESEARCH PAPER

OPEN ACCES

LoRA-LoRaWAN Communication Multinode for 3D Localization in Coastal Environment

Musayyanah[1], Paladie Susanto[1], Pradita Maulidya Efendi[2], Charisma Dimas Affandi[1], Kristin Lebdaningrum[2], and Theodorus Visser Inuliman[1]

[1] Department of Computer Engineering, Universitas Dinamika, Surabaya, Indonesia
[2] Department of Information Systems, Universitas Dinamika, Surabaya, Indonesia

ABSTRACT

The application of LoRaWAN technology in the Internet of Things (IoT) enables real-time communication and efficient data transmission from multiple nodes based on device addresses. LoRaWAN offers long-range communication capabilities, reaching distances of up to several kilometers, at a lower cost compared to high-frequency cellular networks. However, accurate three-dimensional localization remains a challenge in large-scale, low-cost IoT networks. This study addresses this challenge by utilizing LoRaWAN for real-time data communication and three-dimensional localization based on signal strength. Localization begins with an analysis of the path loss model to determine the path loss coefficient. The localization results are transmitted as data packets containing longitude, latitude, altitude, and EN-to-AN distance information to the Things Network (TNN) server using Over The Air Activation (OTAA) mode. This study investigates three-dimensional localization based on signal strength from three LoRa End Nodes (EN) to four LoRa Anchor Nodes (AN), with results forwarded to the Datacakes application. The localization accuracy is evaluated using Root Mean Square Error (RMSE), with values of 169.35 meters for EN1, 395.08 meters for EN2, and 183.24 meters for EN3. Communication performance between the Gateway (GW) and EN is analyzed using Packet Error Ratio (PER), Air Time (AT), and latency, with EN2 showing the best performance: the lowest AT 333.4ms, smallest PER 51%, and lowest latency 10.45 seconds. This indicates that communication closer to the GW improves performance. Future research could explore the integration of additional IoT technologies and further improvements in localization accuracy to support more complex and dynamic environments.

PAPER HISTORY

Received Nov. 15, 2024
Revised Dec. 26, 2024
Accepted Jan. 16, 2025
Published Jan. 25, 2025

KEYWORDS (ARIAL 10)

IoT; LoRAWAN; Localization; OTAA; RMSE; TNN.

CONTACT:

[2]pauladie@dinamika.ac.id

1. INTRODUCTION

The implementation of the Internet of Things [IoT] requires devices with low-power, low-complexity, low-cost, and communicate wirelessly over long distances. Low Power Wide Area Network (LPWAN) is an IoT-based technology that allows real-time data transmission from various devices with low power. One type of LPWAN technology that has been widely studied since 2015 is LoRa, then developed into LoRAWAN in 2018 [1].

LoRAWAN is an IoT connectivity supporter for every IoT implementation case, becoming the most ideal choice for various applications, especially in remote areas. LoRAWAN has the ability to accommodate large amounts of data from thousands of devices within a distance of several kilometers [2]. LoRAWAN is an open-source protocol standardized by the LoRA Alliance that runs on the physical layer of LoRa. The LoRaWAN network architecture consists of end node devices, gateways, servers, and server applications [3]. End node devices are connected to the gateway using a star topology. LoRaWAN forwards messages from end node devices directly to the server in the form of UDP packets. The implementation of LoRAWAN is more economical with a range of up to thousands of kilometers.

Many studies have used LoRAWAN-based IoT technology with cloud server services integrated with user applications, including research for monitoring water quality in rural areas [4], for street lighting [5], monitoring rock debris in coastal areas [6], forest fire alarms [7], and electricity meter measurements [8]. In this article, LoRAWAN is used to accommodate localization data from three end nodes that will later be applied to tracking tourists on the coast.

The application of LoRaWAN sensors and communication devices in coastal or maritime areas was carried out by [9]. LoRa is able to communicate in line of sight (LoS) over the sea as far as 22km, with a relatively linear RSSI value of -50dBm. Furthermore, LoRa is able to communicate in areas with many obstacles or Non LoS with RSSI reaching -100dBm. The performance of GW with LoRa nodes moving over the sea has been analyzed by [10] with a received data ratio packet of around 32% at a maximum distance of 30 km. GW devices and LoRa multihope communication for Telemetry implementation are able to reach 7.6km over the sea [11]. The performance of LoRa as an end node for a shipping monitoring system is able to reach a distance of 3.4km with a packet ratio of 63.26%. These studies conclude

Corresponding author: Pauladie Susanto, pauladie@dinamika.ac.id Department of Computer Engineering Universitas Dinamika, Surabaya, Indonesia.

that LoRa has quite good performance when applied in marine or coastal environments.

Localization with LoRa radio devices is one of the challenges in estimating distance based on signal strength, because LoRa works on ISM frequencies that are quite susceptible to interference. The results of the localization process are position estimation and distance estimation. Position estimation parameters consist of two dimensions (2D) and three dimensions (3D). 2D estimation focuses on the longitude and latitude of the node. 3D estimation predicts the longitude, latitude, and altitude of the node in question. Several studies have implemented three-dimensional LoRa localization techniques based on Received Signal Strength (RSS), outdoors or indoors [12], [13] and [14]. According to [15], localization techniques with time matrices have a better level of accuracy compared to RSS-based localization techniques. Localization with time matrices requires time synchronization from devices that have high specifications and costs [16]. Therefore, RSS-based localization is often applied because it is easier and cheaper. In addition, the results of signal strength-based localization are also influenced by the conditions and area of the observation environment. In [17] localization was carried out in a mountainous area of 100m x 100m, with a localization error of 0.5-10m. The Trilateration concept in LoRa localization was carried out in an area of 200m x 120m, with a localization error of 8.65-21.9m [18].

One of the applications of RSS-based localization techniques to monitor tourist positions was carried out by [19]. The localization technique added the Normalization method with an increase of 15.22%. The localization results can be optimized with the Tapis Kalman signal strength fluctuation reduction method, increasing by 11.7% [20]. The localization results from the above studies were not forwarded to the cloud server for further reach. In this article, the localization results are forwarded to the server application through the LoRa gateway device.

The most crucial and highly influential parameters on RSS-based localization results are the path loss coefficient (n) and the distance obtained from the RSS measurement results. The effect of the LoRa path loss coefficient value on dynamic changes in the reference power measurement results makes the distance estimation more accurate [21]. There are several methods to optimize the n parameter as done by [22], using the deep learning method on n, to improve the estimation accuracy. This article determines the reference power and path loss coefficient from the average RSS LoRa measurement results at several points in the node position observation field using the path loss model as done by [23].

Although RSS-based localization methods in LoRa show promising results for position and distance estimation in coastal areas, there are some limitations that can affect the accuracy and reliability of the results. Localization accuracy can be affected by environmental factors such as weather conditions, terrain, and natural obstacles that can cause signal attenuation or interference, reducing the accuracy of RSS measurements. In addition, LoRa technology has limitations such as signal range being affected by physical obstacles, interference from other devices, and atmospheric conditions, which can cause errors in signal readings and reduce the accuracy of position and distance estimation. Accuracy variations can also occur depending on the density and placement of LoRa nodes, with sparse node placement or lack of reference points leading to larger positioning errors, especially in less dense or less controlled environments. Therefore, the determination of localization parameters is carried out at each observation cluster.

The main objective of this study is to develop and evaluate a method for estimating the position and distance of nodes using the RSS (Received Signal Strength) based localization method on a LoRa network implemented in coastal areas. This study also aims to send the localization results to a cloud platform for further analysis and processing. The localization technique is carried out by the LoRA end node consisting of four Anchor nodes (AN) and 3 End nodes (EN). EN will estimate the position and distance after obtaining reference information in the form of position and RSS from AN, then EN will forward the estimation results to the cloud server. Determination of the parameters n and distance is obtained by conducting point to point measurements of EN, to evaluate changes in the variation of distance values to RSS. This measurement is carried out at several points of the test environment cluster.

The contribution of this article is to process and store localization data on the TNN cloud server, and integrate the data with LoRAWAN-based IoT applications. The testing was carried out in tourism environment in Surabaya, namely Kenjeran Beach Amusement Park. This tourist environment is very appropriate for the needs of LoRAWAN, a fairly large area and crowded with visitors Furthermore, there are areas with different heights that support the three-dimensional localization technique process. The implementation of LoRaWAN does not require expensive costs compared to high-frequency communication systems currently installed in coastal areas such as 4G or 5G cellular technology [11]. The results of this study can be used as a radar or real-time position tracker for tourists or other objects that are used as nodes on the coast..

This paper consists of five parts. Part I reviews the background and objectives of the study. Part II presents the stages of the research method used and the testing scenario. Part III discusses the results of the study. Part IV is a conclusion of the results and suggestions for further research development.

2. METHOD

Corresponding author: Pauladie Susanto, pauladie@dinamika.ac.id Department of Computer Engineering Universitas Dinamika, Surabaya, Indonesia.

Indonesian Journal of Electronics, Electromedical Engineering, and Medical Informatics
Homepage: ijeeemi.org; Vol. 7, No. 1, pp. 11-22, February 2025; e-ISSN: 2656-8624.
https://doi.org/10.35882/ijeeemi.v7i1.46

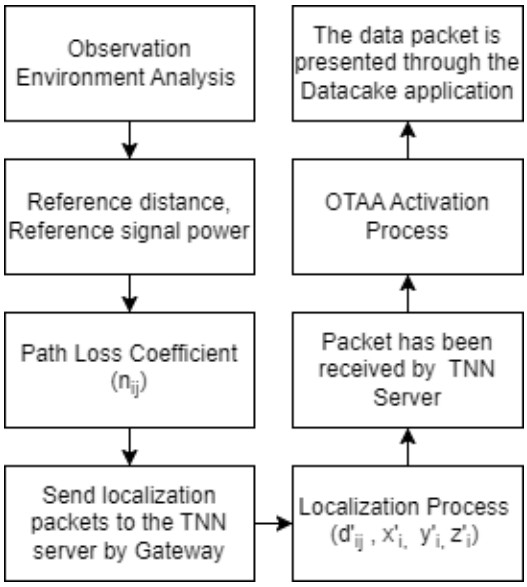

Figure 1. Method Diagram

The overview of the research is shown in Figure. 1. Environmental analysis is used to obtain the pathloss model from the node's position in the coastal environment, followed by the localization process. The results of the localization process are analyzed using the RMSE error method. Subsequently, the localization results are sent to the cloud server TNN to obtain LoRaWAN communication parameters, namely Packet Error Rate (PER), Air Time (AT), and latency.

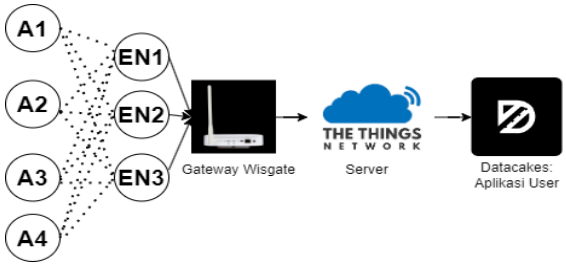

Figure 2. MISO Communication System of LoRA

Figure 2 is a Multiple Input Single Output (MISO) communication system on LoRa for the localization process until the data is forwarded to the server in the form of a UDP packet and then displayed in the application. Multiple inputs from the four ANs as senders of reference position data to EN, using a 4-second scheduling communication algorithm for each AN as in [19]. The payload arrangement received by EN from AN is shown in Figure 3.a. EN will perform localization to obtain the results of its position estimation. Then the estimation results will be sent to The Things Network (TNN) server using OTAA activation mode and displayed in the IoT application. The payload format sent by EN to the Server is shown in Figure 3.b

.

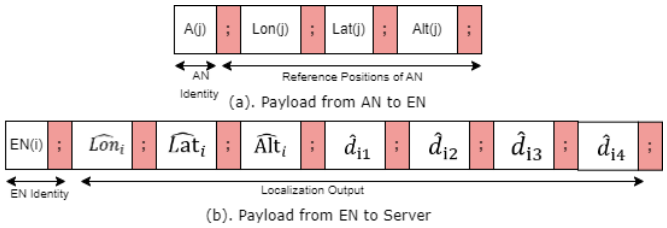

Figure 3. Data Package

The payload from AN to EN consists of the AN identity (AN(j)) along with the 3D position of the relevant AN (Lon(j), Lat(j), Alt(j)). Then EN will detect its position with reference data obtained from AN. The localization results consisted of the EN identity (EN(i)), the three-dimensional localization results ((i), (i), (i)), and the distance between EN and the four ANs (i1), (i2), (i3), (i4)).

The method stages of this research started with environmental analysis to obtain localization reference parameters, namely reference distance and reference power. Then these parameters were used to find the path loss coefficient value. Then the localization process was carried out after the three parameters are obtained. EN was connected to the server using OTAA activation, and the localization data is forwarded to the IoT Platform Datacakes application.

The installation of GW, AN, and EN devices in the observation environment was shown in Figure 3. GW was connected to a laptop to monitor incoming data on the TNN server, EN was connected to a mobile phone to record data from AN and localization results. Data recap from EN used the Serial USB Terminal Application installed on the device. The positions of GW, the four ANs, and the three ENs were measured using a commercial Garmin GPS for analysis of the error rate of localization results.

GW was positioned at the highest place among other nodes, namely the connecting bridge between Lapangan Kenjeran and THP Kenjeran. The three ENs were spread across four clusters. AN was located at Jembatan Suroboyo and THP Kenjeran as in Figure 4.

The microcontrollers installed in AN and EN were high computation microcontroller [24], To support the mathematical process of localization. The GPS sensor installed on AN was the Ubox Neo 6M type [24]. The communication used is the LoRa RF95M type module operating on the 923 MHz frequency band, produced by Hope RF Electronics, installed on EN and AN [25]. The LoRa connection with the server service used a Gateway from RAK Wireless [26]. The frequency settings on LoRa and Gateway use regional rules issued by the LoRa Alliance for Indonesia around 920-923Mhz [27]. This study utilized a free cloud server service from TNN, namely The Things Stack Sandbox [28] and the IoT platform application integrated with TNN is Datacakes [29].

Corresponding author: Pauladie Susanto, pauladie@dinamika.ac.id Department of Computer Engineering Universitas Dinamika, Surabaya, Indonesia.

Indonesian Journal of Electronics, Electromedical Engineering, and Medical Informatics
Homepage: ijeeemi.org; Vol. 7, No. 1, pp. 11-22, February 2025; e-ISSN: 2656-8624.
https://doi.org/10.35882/ijeeemi.v7i1.46

Figure 4. GW, EN and AN installation in test cluster

Environmental Analysis

The first stage of this study was to analyze the coastal environment of tourism in the Kenjeran Beach Entertainment Park (THP), by spreading the AN, EN and GW positions as in Figure 5. The Kenjeran Beach Tourism observed consisted of three areas, namely the Suroboyo Bridge, Kenjeran Field, and Inside the Kenjeran THP. This study divided the test area into 4 observation clusters, namely cluster 1 Suroboyo Bridge, cluster 2 Kenjeran Field, cluster 3 Inside the THP, and cluster 4 Kenjeran Sea. The area of the observation environment is 460 x 215 square meters.

The star notation is the position of the four ANs, the checklist notation is the position of the three ENs, and the dot notation is the position of the GW. The positions of the EN and AN correspond to the Multilateration localization scenario in [30]. The position of the EN must be within the range of the AN cluster, to obtain more accurate localization results. EN1 and EN3 are inside the AN cluster, while EN2 is positioned outside the AN cluster to see the effect of EN2's position on the localization results. The GW is placed in a higher place than the other nodes, so the data from the three ENs can be received as a whole. From each cluster, SISO testing was carried out between ENs, to see the trend of LoRA signal strength values against distance as in Figure 7.

Environmental analysis consised of two stages, namely the first stage was to obtain the reference distance parameters (d_{ref}) and reference signal power (P_{ref}). The dref parameters were obtained from the RSSI measurement results on the 4 clusters with changes in distance, where the measurement results are analyzed using the path loss free spaces equation in Equation (1).

Figure 5. Node Position Scenario

$$FSPL = Pt - 20logd - 20logf - 147.55 \quad (1)$$

Pt is the transmit power of LoRa of 20dBm. The frequency parameter of LoRa is 923 MHz and d is the distance from the two nodes.

The second stage obtained the path loss coefficient (n) and $Pref$ values obtained from the regression equation results of the path loss log normal distance model (2). The set of n values used for the localization process is $n_{ij} \in [n_{i1}, n_{i2}, n_{i3}, n_{i4}]$ = [3.3, 2.95, 2.96, 2.98]. The set of $Pref \in [Pref_{(i1)}, Pref_{(i2)}, Pref_{(i3)}, Pref_{(i4)}]$ = [44.24, 55.57, 51.69, 63.74].

$$y_j = n_j x + Pref_j \quad (2)$$

The n variable is the value of the path loss coefficient, P_{ref} is the reference power in dBm. The variable i is the index of EN, j is the index of AN.

Localization Stage

After getting d_{ref} and P_{ref} from the previous stage, the next stage is the localization process that started from EN receiving the reference position from each AN, then calculating the distance with Equation (3). The localization process was carried out according to Equations (4) – (7).

$$\hat{d}_{ij} = d_{ref}\, 10^{\frac{P_{ref} - P_{RX_{ij}}}{10 n_{ij}}} \quad (3)$$

$$\mathbf{P}_{(3\,x\,1)_i} = \begin{bmatrix} \widehat{Lon}_i \\ \widehat{Lat}_i \\ \widehat{Alt}_i \end{bmatrix} \quad (4)$$

$$\mathbf{Q_{3x3}} = \begin{bmatrix} 2(Lon_1 - Lon_2) & 2(Lat_1 - Lat_2) & 2(Alt_1 - Alt_2) \\ 2(Lon_2 - Lon_3) & 2(Lat_2 - Lat_3) & 2(Alt_2 - Alt_3) \\ 2(Lon_2 - Lon_4) & 2(Lat_2 - Lat_4) & 2(Alt_2 - Alt_4) \end{bmatrix} \quad (5)$$

$$\mathbf{R_{3x1}} = \begin{bmatrix} (Lon_1^2 - Lon_2^2) + (Lat_1^2 - Lat_2^2) + (Alt_1^2 - Alt_2^2) + (\hat{d}_2^2 - \hat{d}_1^2) \\ (Lon_2^2 - Lon_3^2) + (Lat_2^2 - Lat_3^2) + (Alt_2^2 - Alt_3^2) + (\hat{d}_3^2 - \hat{d}_2^2) \\ (Lon_2^2 - Lon_4^2) + (Lat_2^2 - Lat_4^2) + (Alt_2^2 - Alt_4^2) + (\hat{d}_4^2 - \hat{d}_2^2) \end{bmatrix}$$

Corresponding author: Pauladie Susanto, pauladie@dinamika.ac.id Department of Computer Engineering Universitas Dinamika, Surabaya, Indonesia.

Indonesian Journal of Electronics, Electromedical Engineering, and Medical Informatics
Homepage: ijeeemi.org; Vol. 7, No. 1, pp. 11-22, February 2025; e-ISSN: 2656-8624.
https://doi.org/10.35882/ijeeemi.v7i1.46

$$\mathbf{P}_i = \mathbf{Q}^{-1}\mathbf{R} \quad (7)$$

$P_{RX_{i,j}}$ is the power recorded by each AN against EN.d_{ref} The estimated position EN was indicated by the variable **P** and the estimated $\hat{d}_{ij}$ distance was evaluated with the position/distance from the Garmin device in the RMSE Equation (8).

$$RMSE = \sqrt{\frac{1}{n}\sum_{n=0}^{30}(V_{(real)_i} - V_{(est)_i})^2} \quad (8)$$

$V_{(real)_i} \epsilon \{Lon_i, Lat_i, Alt_i, d_{ij}\}$ defines position and distance data by Garmin GPS devices in meters. $V_{est_i} \epsilon \{\widehat{Lon_i}, \widehat{Lat_i}, \widehat{Lat_i}, \hat{d}_{ij}\}$ is the result of localization of longitude, latitude and altitude positions and estimated distance from EN to AN.

Sending Data to the Server

EN and AN devices communicated with each other with regular LoRa without an internet connection, LoRaWAN-based Gateway device was needed to connect it to the server. The Gateway device must first be registered with the TNN server with a server cluster recommended by TNN. In this study, the Gateway was connected to the nearest cluster, namely Australia (au1), to reduce the latency of the IoT activities carried out [31]. The LoRAWAN used in the TNN configuration that was 1.0.3 with class A which supports confirmed and unconfirmed traffic [32]. Confirmed traffic was the GW confirming that the data has been received by the GW, while unconfirmed GW forwards the data to the server without confirmation from the GW. LoRAWAN Version 1.0.3 encrypts AES 128 bit keys on all connected devices, where the encryption key is used to generate the Message Integrity Code (MIC) from LoRAWAN. The MIC form of LoRAWAN can be seen in the JSON file on the TNN server.

The most important part of this process was the EN activation mode and data packet format. Activation Mode in LoRAWAN consisted of OTAA and Activation by Personal (ABP). This article uses OTAA mode, the security level of this mode is better than ABP mode. OTAA always updates its address with different encryption keys from the network server, when the connection is lost [3]. The three ENs are registered in the TNN application with three different keys, namely AppEUI 8 bytes, DevEUI 8 bytes, and AppKey 16 bytes. The keys of AppEUI and DevEUI are the addresses of the device. AppKey is the encryption key to generate a new device address from the EN.

The data packet format sent to the server was as shown in Figure 2. The data packet received by TNN was a string data type. The message types from LoRAWAN were uplink, downlink and application up. The uplink message was a joint-request from OTAA mode. The joint-accept from OTAA was in the downlink message. The application-up message contained data from the EN device sent via GW to the TNN backend application. The maximum payload from LoRAWAN 1.0.3 is 51 bytes, so the payload from the localization results needs to be pre-processed before the data were sent to the server. Technically, using substring syntax for the localization result value behind the comma so that the data did not exceed the LoRAWAN provisions.

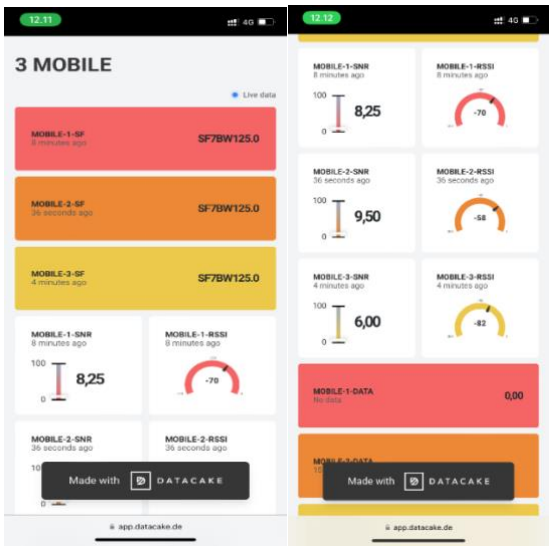

Figure 6. Datacakes mobile app view

JSON data from the server were processed and displayed to the IoT platform integrated with TNN, namely Datacakes. Datacakes is a web and mobile-based IoT application. Each EN was integrated with Datacakes using the API Key from each EN. The data displayed consisted of SNR, RSSI, and the results of the mobile application localization from Datacakes. The display of the three ENs can be seen in Figure 6.

3. RESULTS AND DISCUSSION

The testing in this study was divided into two parts: the results of the localization process and EN communication using LoRaWAN. The localization process involved analyzing the RSSI measurement results from the environment to estimate position and distance. The LoRaWAN communication analysis focused on evaluating LoRaWAN performance, specifically the gateway (GW) in obtaining real-time data from three ENs.

A. Results of Localization Process

The research results started with analyzing the observation environment to obtain reference distance and reference power values. The analysis was carried out from the results of Single Input Single Output (SISO) measurements from LoRa communication with a distance of 1 - 200 meters at several environmental points in Figure 7. The first observation environment (cluster 1) was around the Suroboyo Bridge with the furthest received power value of around -98.38 dBm. The second observation environment (cluster 2) is Kenjeran Field with a received power reaching -102.91dBm. The third observation environment (cluster 3) is the inner area of

Corresponding author: Pauladie Susanto, pauladie@dinamika.ac.id Department of Computer Engineering Universitas Dinamika, Surabaya, Indonesia.

Indonesian Journal of Electronics, Electromedical Engineering, and Medical Informatics
Homepage: ijeeemi.org; Vol. 7, No. 1, pp. 11-22, February 2025; e-ISSN: 2656-8624.
https://doi.org/10.35882/ijeeemi.v7i1.46

THP reaching -102.67dBm. The fourth observation environment (cluster 4) was a measurement cluster from THP to the sea, with the lowest power of -93.61dBm.

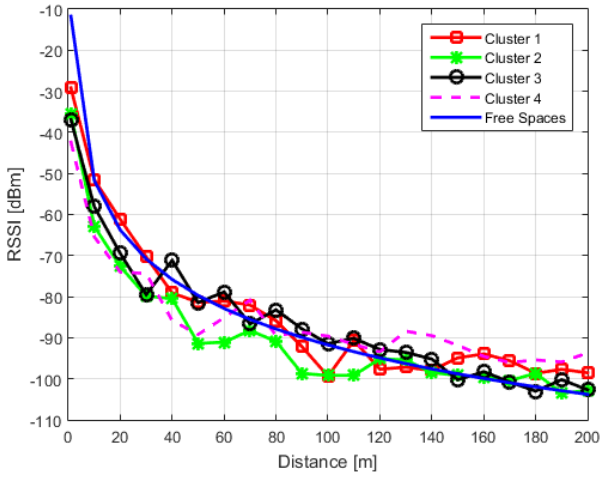

Figure 7. Results of SISI Measurement

The measurement results in Figure 7 showed a pattern of RSSI decline at a longer range. The measurement results were compared with the theoretical results of free space loss equation (1). The environment was surrounded by materials that cause reflections, such as bridges, trees, buildings, the sea and visitors. So that the measurement result graph fluctuates against the free spaces graph. The location points that experience the greatest attenuation are the environment in THP and Kenjeran Field. It is because around the environment there were many kiosk buildings, bridges, trees and crowds of visitors. Fluctuation reduction can be reduced by several filter methods such as in [33] and [34]. Furthermore , fluctuations can be reduced by placing higher position nodes according to the fresnel zone concept, so that signal transmission obtained a path that was freer from obstacles, reduces diffraction and strengthens the signal. The path loss value can be optimized with a deep learning approach [22]. This article optimizes the RSSI value by finding the path loss value from the measurement results.

The SISO measurement results in Figure 8 were processed using linear regression to obtain the n and $Pref$ values as in Figure 7. The first cluster was obtained n1 = 3.30 with $Pref$ = 44.24dBm. The second cluster was obtained n2 = 2.93 with $Pref$ 55.67dBm. The third cluster was obtained n3 = 2.96 with $Pref$ 51.69dBm. The fourth cluster was obtained n4 = 2.28 with $Pref$ = 63.74dBm. The values of the four clusters were used as localization input from AN to EN. According to [35] the reference distance for outdoor environments was around 10-100 meters. This study adopted a dref value of 10 meters. The reference value and path loss coefficient will be used as references in the localization process in equations (3)-(7).

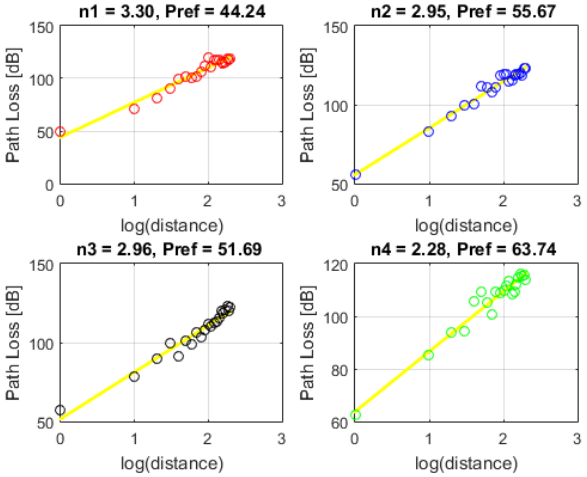

Figure 8. Results for n and Pref Linear Regeression

In addition to the $dref$ and $Pref$ parameters that play an important role in localization, the accuracy of the GPS sensor device, as a reference information provider. The real three-dimensional position of the Garmin device for the entire node AN1 = [12556425.12; 805679.61; 20]. AN2 = [12556370.57; 805480.35; 20]. AN3 = [12556370.57; 805638.42; 27]. AN4 = [12556479.66; 805466.99; 23]. EN1 = [12556469.64; 805659.58; 20]. EN2 = [12556368.34; 805343.43; 13]. EN3 = [12556430.68; 805578.31; 18]. GW = [12556381.70; 805440.28; 52]. The positions represent the sky point, latitude, and altitude. The heights at AN1, AN2, and EN3 were detected to be 20m. According to Figure 5, the three node positions were in the same position cluster. Table I is a comparison of the output of the EN/AN GPS sensor with the Garmin device.

Table 1. RMSE from the Results of GARMIN-GPS

Node	Lon (m)	Lat (m)	Alt (m)
AN1	2.82	2.82	3.00
AN2	4.80	3.350	2.44
AN3	8.60	4.17	22.21
AN4	1.99	0.45	3.53
EN1	1.51	2.52	2.58
EN2	4.58	1.27	32.7
EN3	0.82	1.17	17.58

Table I is the result of the comparison of position detection from GPS sensors to Garmin. According to [36], the standard accuracy of the GPS horizontal value reached 5-10 meters, while for vertical it reached 15-50 meters. The results of the RMSE analysis proved that the accuracy of the sensor device was still within the tolerance range. Furthermore to GPS accuracy, the power captured by EN from AN affects the localization results, the power value was used to calculate the distance estimation parameter ($\hat{d}_{ij}$) as in (3). The distribution of RSSI data from the four ANs to EN1 as shown in Figure 9.

Corresponding author: Pauladie Susanto, pauladie@dinamika.ac.id Department of Computer Engineering Universitas Dinamika, Surabaya, Indonesia.

Indonesian Journal of Electronics, Electromedical Engineering, and Medical Informatics
Homepage: ijeeemi.org; Vol. 7, No. 1, pp. 11-22, February 2025; e-ISSN: 2656-8624.
https://doi.org/10.35882/ijeeemi.v7i1.46

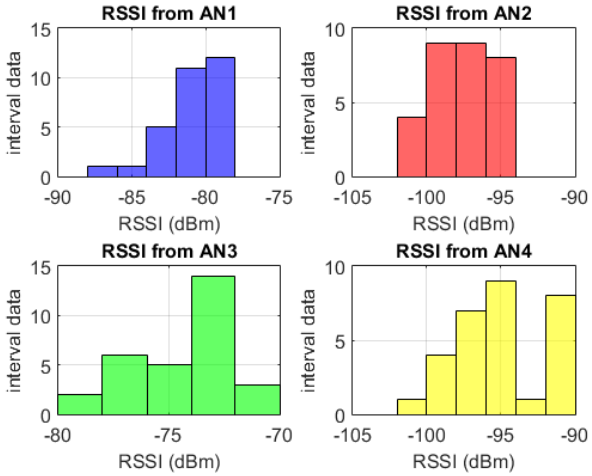

Figure 9. Distribution of RSSI data received by EN1

EN1 received power from AN1 around -75dBm to -90dBm with an average of -81.03dBm. The power captured from AN2 was around -90dBm to -105dBm with an average of -98dBm. The power captured from AN3 was around -70dBm to -80 dBm with an average of -74.70dBm. The power captured from AN4 was around -90dBm to -105dBm with an average RSSI of -95.30dBm. EN1 communication to AN1-AN3 was the strongest signal communication compared to AN2-AN4. The range of EN1 to AN1 and AN3 was closer compared to AN2 and AN4, so there was potential for reflection, interference, or fading phenomena that cause lower received power. The real distance of EN 1 to the four Anchors node consisted of 48.83m, 204.79m respectively; 81.05m, and 192.87m.

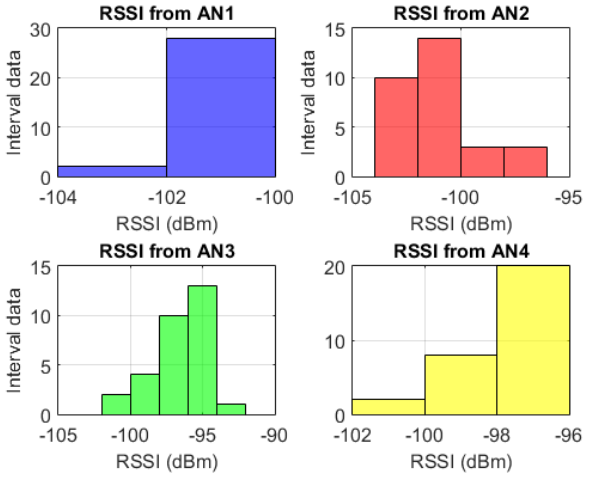

Figure 10. Distribution of RSSI data received by EN2

RSSI distribution from Figure 10 represented the power range received by EN2 from AN1 around -100dBm to -104 dBm, with an average value of -101.60dBm. The power from AN2 is around -95dBm to -105dBm with an average of -101.50dBm. The power from AN3 is at a value of -90dBm to -105dBm with an average of -97dBm. The power from AN4 was -96dBm to -102dBm with the highest value of -97.80dBm. The strongest signal received by EN2 from AN2 because the two node positions are close. While the signals from AN1, AN3 and AN4 decreased. The distance of EN2 to the four Anchors was 341.02m; 137.12m; 345.46m and 166.61m.

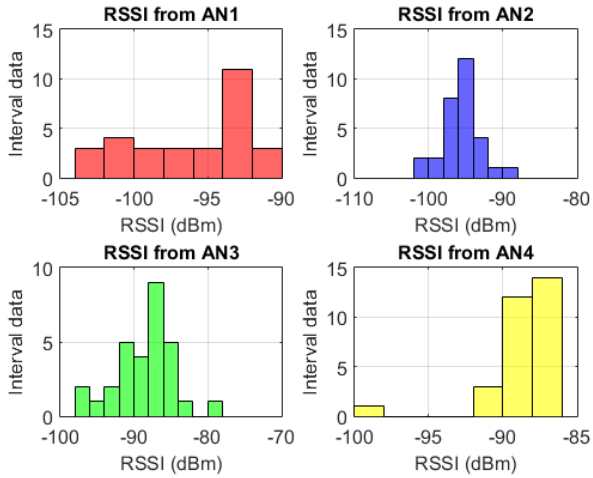

Figure 11. Distribution of RSSI data received by EN3

In Figure 11, EN3 received power from AN1 around -90dBm to -105dBm with an average value of -94.60dBm. Power from AN2 was measured from -80dBm to -110dBm with the highest value of -96dBm. Power from AN3 was measured from -70dBm to -100dBm with an average of -89dBm. Power from AN4 was recorded from -85dBm to -100dBm with an average value of -89dBm. The strongest signals received by EN3 were from AN2 and AN3. The distance of EN3 to the four Anchors consisted of 101.47m; 114.95m; 131.75m and 121.72m.

The overall RSSI data summary received by each EN to AN was still within the RSSI tolerance limit produced by LoRa that was -148dBm. While the practical limit of LoRa reaches -110dBm. These results showed that LoRa communication had decreased in coastal areas, due to reflection or reflection from the sea surface, changing weather or wind conditions affecting antenna polarization and interference from surrounding maritime devices that cause overlap with the ISM frequency of LoRa. Furthermore, interference is caused by reflected waves hitting the ground so that the total signal from the transmitter to the receiver that was weakened [37]. The height of the LoRa device to the ground caused RSSI to fluctuate, thus affecting the estimation results.

The 3D localization result is an estimation parameter consisting of longitude, latitude, altitude and distance. These parameters were compared with the real position of the EN that produces the RMSE value of each estimation parameter shown in Table 2.

Table 2. RMSE position estimation parameter.

NODE	$\widehat{Lon}$ (M)	$\widehat{Lat}$ (M)	$\widehat{Alt}$ (M)	RMSE (M)
EN1	12556446.77	805613.57	126.60	169.35
EN2	12556365.40	805602.32	20.46	395.09
EN3	12556451.06	805572.74	21.72	183.24

Corresponding author: Pauladie Susanto, pauladie@dinamika.ac.id Department of Computer Engineering Universitas Dinamika, Surabaya, Indonesia.

Indonesian Journal of Electronics, Electromedical Engineering, and Medical Informatics
Homepage: ijeeemi.org; Vol. 7, No. 1, pp. 11-22, February 2025; e-ISSN: 2656-8624.
https://doi.org/10.35882/ijeeemi.v7i1.46

The results of the position estimation for the three ENs in Table II show that the lowest RMSE value was 169.35 meters for EN1, 395.09 meters for EN2, and 183.24 meters for EN3. The largest localization error in EN2 was caused by its position being outside the area covered by the four ANs, as shown in Figure 4. According to the concept of Multilateration or Quadlateration localization, the EN's position should ideally be within the AN's coverage area to achieve more accurate localization results. Overall, the RMSE values were still within the tolerance limit of 10% of the total observation area [38].

Table 3. RMSE distance estimation parameter

NODE	$\hat{d}_{i1}$	$\hat{d}_{i2}$	$\hat{d}_{i3}$	$\hat{d}_{i4}$
EN1	10.20	79.14	45.82	10.20
EN2	199.33	28.50	127.64	199.33
EN3	27.11	18.58	42.85	27.11

The RMSE results of the EN distance estimation to AN1, it can be seen that EN2 had a higher distance estimation error compared to other ENs. It is because the distance of EN2 to AN1 was further and was obstructed by bridges, trees, kiosk buildings and sea water so that it affected the distance conversion results. The results of the distance estimation to AN2, the RMSE value of EN1 was higher than the other ENs. It is because the position sof AN2 with EN1 was further away so that it affects the distance conversion results. Similarly, the results of the EN2 distance estimation to AN3 and AN4 were greater than the other ENs. The distance between EN2 to AN3 and AN4 was far and was obstructed by obstacles so that it affected the distance conversion results.

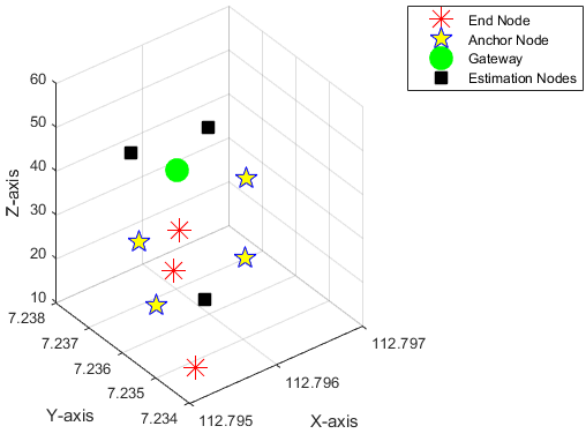

Figure 12. Visualization of 3D localization results

The 3D localization results are shown in Fig. 12, where there is a noticeable distance between the real position and the estimated/localized result. Based on the results of both Tables II and III, it can be concluded that the RSSI-based localization process needs to pay attention to the height of the device to avoid reflections on the ground according to the Fresnel Zone concept or the addition of a method for optimizing the path loss coefficient value, reference power and estimated distance for more optimal results. The localization error rate in Tables II and III can be optimized with other additional RSSI localization algorithms such as Random Neural Network [RNN] [14], applying RSSI fluctuation reduction methods such as Kalman filters [20] - [39], and optimizing the path loss value [40].

B. Analysis of LoRAWN Communication

After obtaining the localization results from Tables II and III, they were forwarded to the TNN server in real time by the three ENs. The ENs were connected to the GW based on the device address, so that the data received from the three ENs were not mixed. The GW will capture RSSI data as an indicator of the strength of the received signal, SNR data to analyze signal quality, Air Time (AT) measured the duration required for LoRAWAN to receive or transmit a signal, and Packet Error Rate (PER) to measure data errors during the transmission process.

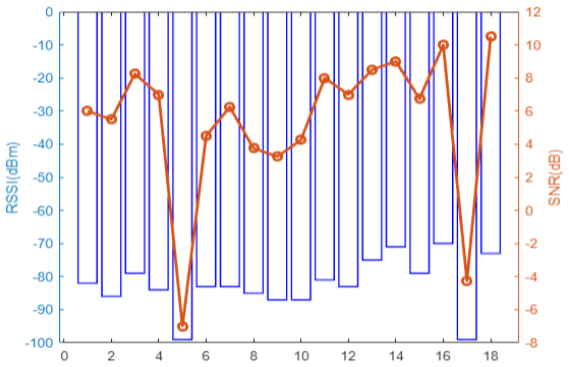

Figure 13. RSSI and SNR from JSON EN1

RSSI and SNR recorded from EN1 application were seen fluctuating with decreasing value in data 5 and 17 simultaneously in Figure 13. RSSI received by EN1 is around -70dBm to -100dBm. SNR recorded was around -10dB to 10dB. Very sharp decrease in RSSI was often followed by less sharp decrease in SNR value. Higher SNR value indicates good quality, while low SNR value means noise in large signal. RSSI value fluctuation was caused by interference or reflection during transmission. This is linear with EN1 position that was far from GW 238.43m.

. The average Air Time (AT) recorded on the server from EN1 was 350.98 ms. The Packet Error Rate (PER) generated by EN1 is 59%. The recorded Spreading Factor (SF) was 7. SF 7 had an SNR Limit of -7.5dB. The results of the smallest recorded SNR data experiment reached -7dB in accordance with the provisions of SF 7. Furthermore, TNN provides a Bandwidth setting of 125kHZ and a Code Rate (CR) of 4/5, allowing error correction from LoRa communication to not be optimal which results in the packet error rate reaching a fairly large value.

LoRAWAN is designed with large latency compared to cellular IoT communications. The use of LoRAWAN is only used for monitoring or tracking positions. The latency of sending data from the EN1 test results to the server is 11.42 seconds. Latency measurements are obtained

Corresponding author: Pauladie Susanto, pauladie@dinamika.ac.id Department of Computer Engineering Universitas Dinamika, Surabaya, Indonesia.

Indonesian Journal of Electronics, Electromedical Engineering, and Medical Informatics
Homepage: ijeeemi.org; Vol. 7, No. 1, pp. 11-22, February 2025; e-ISSN: 2656-8624.
https://doi.org/10.35882/ijeeemi.v7i1.46

from the time data is sent to the time the packet is received on the server.

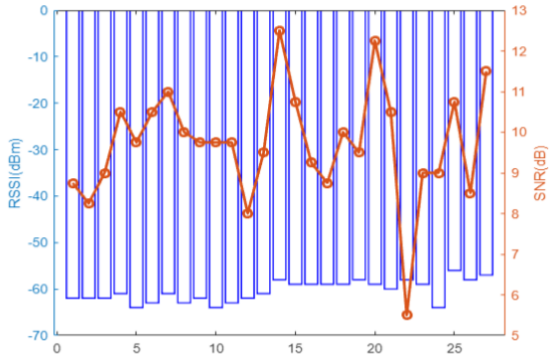

Figure 14. RSSI and SNR from JSON EN2

RSSI recorded on GW for EN2 tends to increase along with the SNR value as seen in Figure 14. In the 14th and 25th data, the SNR and RSSI values were at the highest values of 14dB and -56dBm, indicating that the data were the strongest signal with good quality compared to the other data. While the other values were relatively fluctuating due to environmental conditions with different obstacle materials, namely trees, buildings, and the sea. The distance of EN2 to GW was in accordance with the closer scenario of around 105.56m.

The average Air Time (AT) recorded on the server from EN2 was 333.4 ms with a duty cycle of 1%, so the latency of EN2 was equal to the average Packet Error Rate (PER) of 51%. The distance of EN2 to GW was the closest distance compared to other ENs, allowing more data to be received than other ENs. The recorded Spreading Factor (SF) of EN2 is 7. SF 7 has an SNR Limit of -7.5dB. However, the results of the recorded SNR data experiment reached a positive value, which means it is in accordance with the SNR limit of SF7. In addition, TNN provides a Bandwidth setting of 125kHZ and a Code Rate (CR) of 4/5, allowing error correction from LoRa communication to not be optimal which results in packet errors reaching a fairly large value. However, the PER of EN 2 was better than that of EN1. The average latency of sending EN2 data to the server were 10.45 seconds.

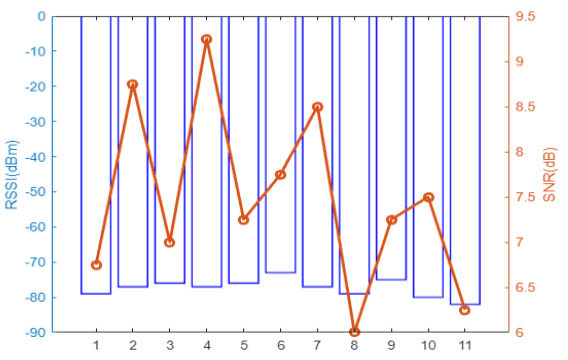

Figure 15. RSSI and SNR from JSON EN3

In Figure 15, the RSSI recorded by GW from EN3 was relatively stable in the range of -70 to -90dBm. While the SNR value fluctuates relatively high, around 6dB to 10dB. At data point 4, the RSSI spikes along with a very sharp decrease in SNR, which means that the increase in signal noise has an impact on the overall signal quality, even though the signal strength value is getting bigger. In data point 7, there was a simultaneous decrease in RSSI and SNR caused by high interference that affects the signal and noise simultaneously. The real distance from EN3 to GW was 105.36m.

The average Air Time (AT) recorded on the server from EN3 was 339.64ms with an average Packet Error Rate (PER) of 67%. SF 7 had an SNR Limit of -7.5dB. However, the results of the recorded SNR data experiment reached a positive value that it is in accordance with the SNR limit of SF7. The distance between EN3 and GW was the second closest distance after EN2, but the AT and PER results were greater, because the location around EN3 was surrounded by a bridge with concrete material, causing the signal strength to decrease and the data received is not optimal. In addition, TNN provides a Bandwidth setting of 125kHZ and Code Rate (CR) 4/5, allowing error correction from LoRa communication to not be optimal which results in packet errors reaching quite large values. The average latency from sending EN3 data to the server were 11.42 seconds. The amount of latency is influenced by signal strength or distance. The latency on EN3 was measured to be the same as EN1. While the distance of EN3 is closer than EN1. It is because the signal strength from EN3 is weakened due to the presence of a bridge obstacle between EN3 and GW, thus affecting the latency value.Tthe communication performance of the three ENs using LoRAWAN, it is proven that LoRAWAN can be relied upon for large-scale IoT applications.

4. CONCLUSION

The results of the application of RSSI-based localization techniques on LoRa communications on the coast with four Anchor Nodes and three End Nodes, consist of the estimated position of EN and the distance of EN to AN. The results of the estimated localization position on EN1 was 169.35 meters, EN2 was 395.09 meters and EN3 was 183.24 meters. The estimated distances of the three ENs to AN1 were respectively 10.20 meters; 199.33 meters and 27.11 meters. The estimated distances of the three ENs to AN2 were respectively 79.14 meters; 28.50 meters and 18.58 meters. The estimated distances of the three ENs to AN3 were 45.82 meters; 127.64 meters and 42.85 meters. The estimated distances of the three ENs to AN4 were 10.20 meters; 199.33 meters and 27.11 meters.

.Factors affected the results of signal strength-based localization include RSSI fluctuations, node heights, and ISM LoRa frequency interference. Fluctuations occurred due to the phenomenon of reflection around the observation environment. Node heights that did not match the Fresnel Zone. Interference in the ISM LoRa frequency band occurs during testing.

Corresponding author: Pauladie Susanto, pauladie@dinamika.ac.id Department of Computer Engineering Universitas Dinamika, Surabaya, Indonesia.

The localization results forwarded to the cloud server were successfully received and displayed on the Datacakes application. The results were added to the analysis of the communication parameters of the GW device with EN, namely RSSI, SNR, Air Time and Packet Error Rate. The test results stated that the strongest signal strength with high SNR occurred in the communication between GW and EN2, because the distance between the two was closer than the other ENs. The smallest Packet Error Rate parameter occurred in the transmission process from EN2 to GW. The lowest latency from the test results was experienced by EN2.

It is expected that for further research to improve the localization results with the other methods such as Weighted Least Square (WLS), and Dynamics Accuracy Estimation (DAE). The improvement of localization errors needs to be given fluctuation reduction methods from RSSI resulting from LoRa communication measurements such as Kalman filters. Optimal towards determining the value of path loss coefficient and distance conversion from RSSI. As well as need to be considered in the determination of the placement of the position of the node or the height of the node against the ground.

REFERENCES

[1] J. Haxhibeqiri, E. De Poorter, I. Moerman, and J. Hoebeke, “A survey of LoRaWAN for IoT: From technology to application,” *Sensors (Switzerland)*, vol. 18, no. 11, 2018, doi: 10.3390/s18113995.

[2] F. Adelantado, X. Vilajosana, P. Tuset-Peiro, B. Martinez, J. Melia-Segui, and T. Watteyne, “Understanding the Limits of LoRaWAN,” *IEEE Commun. Mag.*, vol. 55, no. 9, pp. 34–40, 2017, doi: 10.1109/MCOM.2017.1600613.

[3] M. A. Ertürk, M. A. Aydın, M. T. Büyükakkaşlar, and H. Evirgen, “A Survey on LoRaWAN Architecture, Protocol and Technologies,” *Futur. Internet*, vol. 11, no. 10, p. 216, 2019, doi: 10.3390/fi11100216.

[4] W. A. Jabbar *et al.*, “Development of LoRaWAN-based IoT system for water quality monitoring in rural areas,” *Expert Syst. Appl.*, vol. 242, no. May 2022, p. 122862, 2024, doi: 10.1016/j.eswa.2023.122862.

[5] S. M. M. S. Zakaria *et al.*, “Design and deployment of LoRaWAN smart streetlight for smart city,” 2022, doi: https://doi.org/10.1063/5.0192569.

[6] M. Ragnoli, A. Leoni, G. Barile, V. Stornelli, and G. Ferri, “LoRa Structural Monitoring Wireless Sensor Networks,” in *International Conference on Sensor Network (SENSORNET)*, 2023, no. 12, pp. 79–86, doi: 10.5220/0011692100003399.

[7] T. P. Truong, Q. T. Tran, and P. T. Le, “Design and implementation of a LoRa-based system for warning of forest fire,” *Telkomnika (Telecommunication Comput. Electron. Control.*, vol. 21, no. 5, pp. 1113–1120, 2023, doi: 10.12928/TELKOMNIKA.v21i5.24712.

[8] Sugianto, R. Harwahyu, A. Al Anhar, and R. F. Sari, “Simulation of mobile LoRa gateway for smart electricity meter,” *Int. Conf. Electr. Eng. Comput. Sci. Informatics*, vol. 2018-Octob, pp. 292–297, 2018, doi: 10.1109/EECSI.2018.8752818.

[9] N. Jovalekic, V. Drndarevic, E. Pietrosemoli, I. Darby, and M. Zennaro, “Experimental study of LoRa transmission over seawater,” *Sensors (Switzerland)*, vol. 18, no. 9, pp. 1–23, 2018, doi: 10.3390/s18092853.

[10] J. Petäjäjärvi, K. Mikhaylov, A. Roivainen, T. Hänninen, and M. Pettissalo, “On the coverage of LPWANs: Range evaluation and channel attenuation model for LoRa technology,” *2015 14th Int. Conf. ITS Telecommun. ITST 2015*, no. December, pp. 55–59, 2016, doi: 10.1109/ITST.2015.7377400.

[11] O. Puspitorini, H. Mahmudah, A. Wijayanti, and N. A. Siswandari, “Implementasi Telemetri dan Evaluasi Performansi Sistem Komunikasi Lora di Daerah Pesisir Pantai,” *ELKOMIKA J. Tek. Energi Elektr. Tek. Telekomun. Tek. Elektron.*, vol. 11, no. 1, p. 180, 2023, doi: 10.26760/elkomika.v11i1.180.

[12] E. Svertoka, A. Rusu-Casandra, R. Burget, I. Marghescu, J. Hosek, and A. Ometov, “LoRaWAN: Lost for Localization?,” *IEEE Sens. J.*, vol. 22, no. 23, pp. 23307–23319, 2022, doi: 10.1109/JSEN.2022.3212319.

[13] H. R. Zhu, Hongxu.; Tsang, K.F; Liu, Yucheng.; Wei, Yang.; Wang, Hao.; Wu, C.K.; Chi, “Extreme RSS Based Indoor Localization for LoRaWAN with Boundary Autocorrelation,” *IEEE Trans. Ind. Informatics*, vol. 17, no. 7, pp. 4458–4468, 2021, doi: 10.1109/TII.2020.2996636.

[14] E. P. Godoy, “Improved Indoor 3D Localization using LoRa Wireless Communication,” *IEEE Lat. Am. Trans.*, vol. 20, no. 3, pp. 481–487, 2022, doi: 10.1109/TLA.2022.9667147.

[15] L. E. Marquez and M. Calle, “Understanding LoRa-Based Localization: Foundations and Challenges,” *IEEE Internet Things J.*, vol. 10, no. 13, pp. 11185–11198, 2023, doi: 10.1109/JIOT.2023.3248860.

[16] R. Mani, A. Rios-Navarro, J.-L. Sevillano-Ramos, and N. Liouane, “Improved 3D localization algorithm for large scale wireless sensor networks,” *Wirel. Networks*, vol. 0, 2023, doi: 10.1007/s11276-023-03265-0.

[17] G. M. Bianco, R. Giuliano, G. Marrocco, F. Mazzenga, and A. Mejia-Aguilar, “LoRa System for Search and Rescue: Path-Loss Models and Procedures in Mountain Scenarios,” *IEEE Internet Things J.*, vol. 8, no. 3, pp. 1985–1999, 2021, doi: 10.1109/JIOT.2020.3017044.

[18] A. Mackey and P. Spachos, “LoRa-based Localization System for Emergency Services in GPS-less Environments,” *INFOCOM 2019 - IEEE Conf. Comput. Commun. Work. INFOCOM WKSHPS 2019*, no. October, pp. 939–944, 2019, doi: 10.1109/INFCOMW.2019.8845189.

[19] Musayyanah, P. Kristalina, Y. Triwidayastuti, P.

Corresponding author: Pauladie Susanto, pauladie@dinamika.ac.id Department of Computer Engineering Universitas Dinamika, Surabaya, Indonesia.

Susanto, and M. Z. S. Hadi, "Distributed localization using normalized quadlateration in LoRa networks: application for tourist position estimation," *Indones. J. Electr. Eng. Comput. Sci.*, vol. 29, no. 3, pp. 1446–1455, 2023, doi: 10.11591/ijeecs.v29.i3.pp1446-1455.

[20] M. MUSAYYANAH, C. D. AFFANDI, and K. LEBDANINGRUM, "Penerapan Filter Kalman untuk Estimasi Jarak dan Posisi pada Lokalisasi Outdoor berbasis RSSI dengan Komunikasi LoRa," *ELKOMIKA J. Tek. Energi Elektr. Tek. Telekomun. Tek. Elektron.*, vol. 11, no. 4, p. 849, Oct. 2023, doi: 10.26760/elkomika.v11i4.849.

[21] H. Vo, V. H. L. Nguyen, V. L. Tran, F. Ferrero, F. Y. Lee, and M. H. Tsai, "Advance path loss model for distance estimation using LoRaWAN network's Received Signal Strength Indicator (RSSI)," *IEEE Access*, vol. PP, p. 1, 2024, doi: 10.1109/ACCESS.2024.3412849.

[22] M. O. Ojo, I. Viola, S. Miretti, E. Martignani, S. Giordano, and M. Baratta, "A Deep Learning Approach for Accurate Path Loss Prediction in LoRaWAN Livestock Monitoring," *Sensors*, vol. 24, no. 10, p. 2991, 2024, doi: 10.3390/s24102991.

[23] H. Kwasme and S. Ekin, "RSSI-based localization using LoRAWAN technology," *IEEE Access*, vol. 7, pp. 99856–99866, 2019, doi: 10.1109/ACCESS.2019.2929212.

[24] Arduino, "Arduino Due," *2024*. https://docs.arduino.cc/hardware/due/.

[25] HopeRF Electronic, "RFM95/96/97/9(W)-Low Power Long Range Tranceiver Module V1.0," vol. 98. [Online]. Available: http://www.hoperf.com.

[26] RAK, "RAK7268V2 / RAK7268CV2 WisGate Edge Lite 2 Datasheet Overview Description Specifications Overview." .

[27] LoRa™ Alliance, "LoRaWAN™ Regional Parameters v1.1rA," *LoRaWAN™ 1.1 Specif.*, p. 56, 2017, [Online]. Available: https://lora-alliance.org/sites/default/files/2018-05/lorawan-regional-parameters-v1.1ra.pdf.

[28] T. T. Industries, "LoRAWAN." https://www.thethingsindustries.com/docs/getting-started/lorawan-basics/ (accessed Feb. 19, 2024).

[29] datacakes, "Datacake Low-Code IoT Platform," 2024. https://datacake.co/.

[30] F. Mekelleche and H. Haffaf, "Classification and Comparison of Range-Based Localization Techniques in Wireless Sensor Networks," *J. Commun.*, vol. 12, no. 4, pp. 221–227, 2017, doi: 10.12720/jcm.12.4.221-227.

[31] The Things Industries, "The Things Stack Cloud-Cluster," *2024*, 2024. https://www.thethingsindustries.com/docs/the-things-stack/cloud/.

[32] S. Javed and D. Zorbas, "A LoRaWAN Adaptive Retransmission Mechanism," *2023 IEEE Conf. Stand. Commun. Networking, CSCN 2023*, pp. 324–327, 2023, doi: 10.1109/CSCN60443.2023.10453118.

[33] F. M. Wibowo and A. Burhanuddin, "PENERAPAN KALMAN FILTER PADA METODE TRILATERASI UNTUK PENINGKATAN AKURASI ESTIMASI PERHITUNGAN JARAK DI DALAM RUANGAN," *J. Ilm. Betrik Vesemah Teknol. Inf. dan Komput.*, vol. 09, no. 02, pp. 96–102, 2018.

[34] I. Ullah, X. Su, J. Zhu, X. Zhang, D. Choi, and Z. Hou, "Evaluation of Localization by Extended Kalman Filter , Unscented Kalman Filter , and Particle Filter-Based Techniques," *Wirel. Commun. Mob. Comput.*, vol. 2020, 2020, doi: https://doi.org/10.1155/2020/8898672.

[35] P. Mubarokah, L., Handayani, "Karakteristik Redaman dan Shadowing dalam Ruang pada Kanal Radio 2,4 GHz.," *J. Tek. ITS*, vol. 4, no. 1, pp. 25–30, 2015.

[36] G. S. Center, "Accuracy of distance/speed readings," 2024. https://support.garmin.com/en-IN/?faq=IcyYpjUzRZ8vwH6C107CE8.

[37] R. Thalib Putra *et al.*, "Pengaruh Interferensi Sistem Komunikasi Lora Pada Fresnel Zone Antara End Device Dengan Gateway," *J. Electr. Eng. Energy, Inf. Technol.*, vol. 10, no. 2, pp. 1–12, 2022, [Online]. Available: http://dx.doi.org/10.26418/j3eit.v10i2.60758.

[38] A. Pratiarso, A. S. Putra, P. Kristalina, A. Sudarsono, M. Yuliana, and I. G. P. Astawa, "Skema Lokalisasi Posisi Node Terdistribusi pada Lingkungan Free Space Path Loss," *J. Nas. Tek. Elektro dan Teknol. Inf.*, vol. 6, no. 3, pp. 352–358, 2017, doi: 10.22146/jnteti.v6i3.338.

[39] H. Kausa and S. Chattaraj, "On some issues in Kalman filter based trilateration algorithms for indoor localization problem," 2022, doi: 10.1109/SPICES52834.2022.9774037.

[40] Giulio Maria Bianco; Romeo Giuliano; Gaetano Marrocco; Franco Mazzenga; Abraham Mejia-Aguilar, "LoRa System for Search and Rescue: Path-Loss Models and Procedures in Mountain Scenarios," *IEEE Internet Things J.*, vol. 3, pp. 1985–1999, 8AD, [Online]. Available: https://ieeexplore.ieee.org/document/9169667.

Corresponding author: Pauladie Susanto, pauladie@dinamika.ac.id Department of Computer Engineering Universitas Dinamika, Surabaya, Indonesia.

AUTHOR BIOGRAPHY

Musayyanah obtained a bachelor's degree in telecommunications engineeringPoliteknik Elektronika Surabaya (PENS). She also obtained a Master of Engineering degree in 2015 from Institut Teknologi Sepuluh Nopember. Currently, she is a lecturer in the Department of Computer Engineering, Faculty of Information and Technology (FTI), Universitas Dinamika, Surabaya Indonesia researching wireless sensor networks and the internet of things. She has one scope-indexed publication with 2 citations. G-scholar publications with h-index of 6.

Pauladie Susanto obtained bachelor's degree at Universitas Dinamika. He obtained master's degree at Institut Teknologi Sepuluh Nopember. Currently, he is a lecturer in the Department of Computer Engineering, Faculty of Information and Technology (FTI), Universitas Dinamika, Surabaya Indonesia. He conducts research on wireless sensor network, automation and internet of things. He has several National and International publications. He has one scope-indexed publication with 9 citations. G-scholar publications with h-index of 1.

Pradita Maulidya Effendi earned a bachelor's degree in computer science at the Universitas Dinamika, majoring in Information Systems in 2016, then continued her master's degree in Institut Teknologi Sepuluh Nopember and graduated in 2019. Currently, he is interested in research on the development of Information Technology related to learning, especially learning evaluation at the secondary education level, which also includes programming, system analyst, data analyst, UI/UX, and human-computer interaction.

Charisma Dimas Affandi graduated with a Bachelor of Engineering degree from Universitas Dinamika (STIKOM Surabaya) in 2020. Currently, he works at Universitas Dinamika (STIKOM Surabaya) as a Laboratory Staff at the Faculty of Technology and Informatics. His research focuses include the Internet of Things (IoT), automation, networking, robotics, and image processing.

Kristin Lebdaningrum graduated in Information System from STIKOM Surabaya in 2017. She was a laboratory attendant and lecturer assistant in the department of Information Technology between 2018 and 2022. She taught programming fundamental languages such as Java, PHP, MySQL, HTML, and SQL especially in Oracle Database. she moved to in the Research Department became to a section editor in order to journal research publication. She has truly interested to research area.

Theodorus Visser Inulimang earned his Bachelor of Engineering (S.T.) degree in Computer Engineering from the Faculty of Information Technology, Universitas Dinamika, Surabaya, Indonesia, in 2024. During his studies, he served as a teaching assistant.

Corresponding author: Pauladie Susanto, pauladie@dinamika.ac.id Department of Computer Engineering Universitas Dinamika, Surabaya, Indonesia.